OPTICAL FIBER TECHNOLOGY **2**, 143–148 (1996)
ARTICLE NO. 0016

Femtosecond Soliton Amplification in an Er-Doped Fiber Amplifier with Inhomogeneously Broadened Line

E. MARTÍ-PANAMEÑO*

Facultad de Ciencias Físico-Matemáticas, Benemérita Universidad Autónoma de Puebla, Apdo. Postal 1704, 72001 Puebla, Mexico

V. A. VYSLOUKH, M. TORRES-CISNEROS, AND J. J. SÁNCHEZ-MONDRAGÓN

Instituto Nacional de Astrofísica, Optica y Electrónica, Tonantzintla, Mexico

AND

G. E. TORRES-CISNEROS

Facultad de Ingeniería Mecánica, Eléctrica y Electrónica, Universidad de Guanajuato, Mexico

Received September 5, 1995; revised January 5, 1996

We report a new theoretical approach—the spectral perturbations method—which offers opportunities to analyze the evolution of the femtosecond soliton parameters in fiber amplifiers with inhomogeneously and homogeneously broadened lines. We show that the physical mechanism of the amplification line broadening does not affect significantly the output soliton parameters provided that the saturation effect is negligible. Analytical results are supported by computer simulations.

1. INTRODUCTION

In recent years great advantages of on-line amplification with the help of erbium-doped fiber amplifiers (EDFAs) in a high-speed fiber communication lines have been persuasively demonstrated. In theoretical and experimental research on EDFAs it is possible to detect at least two directions: the main one is related to the implementation of EDFAs as on-line amplifiers in all optical fiber communication lines to achieve multi-gigabit per second pulse train propagation for several thousands of kilometers. Experiments show that EDFAs allow practically error free transmission. The use of EDFA with inhomogeneously broadened line (IBL) yields the amplification of frequency multiplexed signals. Pulse trains with different carrier frequencies can be almost independently amplified in EDFAs with IBL because different signals are in resonance with different groups of active ions. The wavelength division multiplexing techniques could offer significant economic performance advantages for a network through improved capacity, reliability, and transparency. An extended list of publications on this topic is presented in [1–3].

The second research line related to EDFAs is in femtosecond laser systems, where they play different roles either as active elements in lasers or as external elements for further amplification and time compression of emitted laser pulses [4, 5]. The application of EDFAs with IBL opens the possibility of new complementary implementations, for example, the simultaneous generation and amplification of solitons with different carrier frequencies. This activity is very promising for a time domain spectroscopy of ultrafast phenomena.

The mathematical description of the soliton pulse amplification process in the range of hundreds of femtosecond duration is well developed for amplifiers with homogeneously broadened line (HBL) [6–8]; however, it is not quite clear for soliton-like pulses in a fiber amplifier with a significant inhomogeneous component.

In this paper we propose a new theoretical approach, the spectral perturbation method, which gives us the opportunity to analyze the amplification dynamics of femtosecond solitons in a fiber amplifier with inhomogeneously broadened gain line. Results of computer simulation based on direct numerical integration of the nonlinear Schrödinger equation coupled with corresponding equations for nonlinear polarization are also presented.

2. THE MATHEMATICAL MODEL

The mathematical description of the ultrashort pulse amplification in an active fiber medium is based on the nonlinear Schrödinger equation for the dimensionless complex amplitude

* FAX (52)-22-33 24 03. E-mail: emarti@fcfm.buap.mx.

1068-5200/96 $18.00

of the pulse envelope $q(z, \tau)$ (see e.g. [6]):

$$i\frac{\partial q}{\partial z} = \frac{1}{2}\frac{\partial^2 q}{\partial \tau^2} + (1-\beta)|q|^2 q + \beta Q q + i\frac{1}{2}GP. \quad (1)$$

In this equation the first term on the right-hand side describes the pulse dispersion spreading, the second term describes the electronic nonlinearity (Kerr effect), the third term describes the Raman contribution to the nonlinear polarization, and the last term describes the active Er^{3+} ions contribution (the gain term). The running time $\tau = (t - z/u)$ is normalized to the input pulse duration τ_0; u is the group velocity. The distance z is normalized to the dispersion length $L_d = \tau_0^2/|k_2|$, with $k_2 = \partial^2 k/\partial\omega^2$, where $k(\omega)$ is the mode propagation constant.

The complex amplitude q is expressed in the units of the one-soliton pulse amplitude with the duration τ_0:

$$|q_s^0| = \sqrt{8\pi k_2/(\tau_0^2 k_0 \tilde{n}_2 c n_0)},$$

where $\tilde{n}_2 = 3.2 \times 10^{-16}$ cm^2/W is the nonlinear coefficient, n_0 is the refractive index. The parameter $\beta \approx 0.2$ determines the Raman contribution to the nonlinear refractive index. The amplification parameter $G = L_d/L_a$, where L_a is the amplification length [6].

The dynamics of the molecular oscillations induced by ultrashort pulses is governed by the equation for the real amplitude Q:

$$\mu^2\frac{\partial^2 Q}{\partial \tau^2} + 2\mu\delta\frac{\partial Q}{\partial \tau} + Q = |q|^2. \quad (2)$$

Here $\mu = (\tau_0\Omega_R)^{-1}$, $\delta = (T_2^R\Omega_R)^{-1}$, where Ω_R is the Raman resonant frequency, and $T_2^R = 1/(\pi\Delta\nu_R)$ is corresponding characteristic time, $\Delta\nu_R$ is the Raman line bandwidth. For silica glass fiber typical values of these parameters are $\Omega_R \simeq 83$ THz, $\Delta\nu_R \simeq 7.5$ THz, $T_2 \simeq 50$ fs. The amplitude Q is expressed in the units $Q_n = \chi_Q'|q_s|^2/4M\Omega_R^2$, with $\chi_Q' = \partial\chi/\partial Q$, where χ is the electronic polarizability of the molecule which depends on Q parametrically and M is the effective molecule mass.

Considering the process of amplification of the femtosecond soliton it is necessary to take into account that the one-soliton energy density ($\sim 10^{-4}$ J/cm^2) is several orders lower than the saturation energy density of the resonant transition (~ 10 J/cm^2), so the variation of the laser transition population is negligible. In the case of homogeneous broadening we can write the following equation for the ion polarization complex amplitude:

$$\gamma_a\frac{\partial P}{\partial \tau} + (1 + i\gamma_a\Delta)P = q. \quad (3)$$

The complex amplitude P has been normalized to the value $P_n = d^2 N_0|q_s^0|^2/\hbar$, where d is the dipole moment of the resonant transition, N_0 is the density of the poupulation inversion created by the pump, $\gamma_a = T_2/\tau_0$ is the normalized dipole decay time which is related to the width of the homogeneous line by the formula $T_2 = 1/(\pi\Delta\nu_h)$. For different doping component the value of $\Delta\nu_h$ varies within the interval 0.54–1.5 THz (18–50 cm^{-1}) [3]. The parameter $\Delta = (\omega_0 - \omega_{12})\tau_0$ is the normalized soliton carrier frequency detuning from the resonance transition frequency ω_{12}.

In a spectral domain Eq. (3) describes an amplification line with the Lorentzian contour:

$$P(\Omega) = \frac{q(\Omega)}{1 - i\gamma_a(\Omega - \Delta)}. \quad (4)$$

For Al_2O_3:SiO_2 core optical fibers the line broadening is mainly homogeneous but for GeO_2:SiO_2 core fibers inhomogeneous broadening dominates [3]. In the latter case the spectrum of the resonant polarization can be expressed as the average of Eq. (4) over the inhomogeneous line contour $g(\Delta)$:

$$P(\Omega) = q(\Omega)\int_{-\infty}^{\infty}\frac{g(\Delta)}{1 - i\gamma_a(\Omega - \Delta)}d\Delta. \quad (5)$$

Notice that Eq. (5) represents a convolution of the Lorentzian line with the spectral distribution of the active ions. In the time domain the polarization complex amplitude $P(\tau)$ can be obtained as the inverse Fourier transformation of Eq. (5):

$$P(\tau) = \frac{1}{2\pi}\iint_{-\infty}^{\infty}\frac{g(\Delta)q(\Omega)\exp(-i\Omega\tau)}{1 - i\gamma_a(\Omega - \Delta)}d\Delta\, d\Omega. \quad (6)$$

For computer simulation we used the Gaussian line shape

$$g(\Delta) = \frac{1}{\sqrt{2\pi}\sigma}\exp\left(-\frac{\Delta^2}{2\sigma^2}\right), \quad (7)$$

where σ is the semiwidth of the IBL; it is related to the characteristic time T_2^* by the formula $\sigma = (\sqrt{2\ln 2}T_2^*)^{-1}$. A typical value of the inhomogeneous width is of the order of 50 cm^{-1} [3].

Finally we highlight that the effect of IBL can be remarkable in the amplification of soliton pulse trains with a high repetition frequency. In this case the saturation effect plays an important role and a spectral hole burning may be essential.

3. SPECTRAL PERTURBATIONS OF OPTICAL SOLITON

It is well known that the unperturbed Schrödinger equation (Eq. (1) in the case $\beta = 0$, $G = 0$) has the one-soliton solution which can be written as

$$q_s(z, \tau) = \kappa\,\mathrm{sech}[\kappa(\tau - \tau_s) + \Omega_s z]\exp[i\Phi(z, \tau)], \quad (8)$$

$$\Phi(z, \tau) = \Omega_s(\tau - \tau_s) - (\kappa^2 - \Omega_s^2)z/2 + \phi_s,$$

where κ is the form factor determining the soliton amplitude and its duration, Ω_s is the normalized central frequency, τ_s is the time coordinate of the soliton center, ϕ_s is the initial phase. In the case of the perturbed Schrödinger equation the soliton parameters should be treated as functions of evolution variable z: $\kappa = \kappa(z)$, $\Omega_s = \Omega_s(z)$, $\tau_s = \tau_s(z)$, $\phi_s = \phi_s(z)$.

Raman contribution to the nonlinear polarization $\sim \beta Qq$ usually acts as a small perturbation and it does not change the soliton form factor ($\delta\kappa^R = 0$ at least in the frame of the first order approximation) but causes monotonic in z red self-frequency shift which strongly depends on the form factor [9]

$$\delta\Omega_s^R = -\frac{8}{15}\sigma\kappa^4 dz, \tag{9}$$

where the parameter $\sigma = 2\beta\mu\gamma$.

If the amplification parameter $G = L_d/L_a$ satisfies the inequality $G \ll 1$, this means that the soliton energy increment at the distance of one dispersion length is relatively small, and the last term in Eq. (1) can also be treated as perturbing one. Such a situation is typical only for femtosecond solitons. Then the complex amplitude variation δq resulting from passing a small distance dz can be written as

$$\delta q(z,\tau) = \frac{1}{2}GP(z,\tau)dz, \tag{10}$$

where $P(z,\tau)$ is governed by Eq. (5) assuming $q = q_s(z,\tau)$. To calculate appropriate variations of the soliton parameters $\delta\kappa$, $\delta\Omega_s$ one can use the known integral relations in a time domain [10]:

$$\delta\kappa = \kappa\int_{-\infty}^{\infty}\operatorname{sech}(\kappa\tau)\Re[\exp(-i\Omega_s\tau)\delta q(\tau)]\,d\tau, \tag{11}$$

$$\delta\Omega_s = \kappa\int_{-\infty}^{\infty}\operatorname{sech}(\kappa\tau)\tanh(\kappa\tau)\Im[\exp(-i\Omega_s\tau)\delta q(\tau)]\,d\tau. \tag{12}$$

But in the problem under consideration relations between $\delta\kappa$, $\delta\Omega_s$, and δq are more conveniently expressed in a spectral domain. Substituting the inverse Fourier transform of $\delta q(\tau)$,

$$\delta q(\tau) = \int_{-\infty}^{\infty}\delta q(\Omega)\exp(i\Omega\tau)\,d\Omega, \tag{13}$$

into Eqs. (11) and (12) and evaluating interior integrals over τ we obtain

$$\delta\kappa = \pi\int_{-\infty}^{\infty}\operatorname{sech}\left[\frac{\pi(\Omega-\Omega_s)}{2\kappa}\right]\Re[\delta q(\Omega)]\,d\Omega, \tag{14}$$

$$\begin{aligned}\delta\Omega_s &= 2\int_{-\infty}^{\infty}\left[\frac{\pi(\Omega-\Omega_s)}{2\kappa}\right]\\ &\quad\times\operatorname{sech}\left[\frac{\pi(\Omega-\Omega_s)}{2\kappa}\right]\Re[\delta q(\Omega)]\,d\Omega.\end{aligned} \tag{15}$$

So, the form factor variation $\delta\kappa$ is proportional to the overlap integral of the soliton spectral amplitude $q_s(\Omega) = (1/2)\operatorname{sech}[\pi(\Omega-\Omega_s)/2\kappa]$ with the spectral amplitude of perturbation $\delta q(\Omega)$. The soliton frequency variation $\delta\Omega_s$ is proportional to the first moment of the same overlap integral about the point $\Omega = \Omega_s$.

Taking into account Eqs. (5) and (10) we express the real part of the spectral perturbation as

$$\Re[\delta q(\Omega)] = \frac{1}{2}Gdz\, q_s(\Omega)\int_{-\infty}^{\infty}\frac{g(\Delta)}{1+\gamma_a^2(\Omega-\Delta)^2}\,d\Delta. \tag{16}$$

Using Eq. (16) and Eqs. (14) and (15) one can easily calculate variations of the soliton parameters by numerical integration, but some important particular cases can be treated analytically. For example, if inhomogeneous broadening dominates over homogeneous broadening then $T_2^* \ll T_2$ and the pulse is relatively short $\tau_0 \ll T_2$ ($\gamma_a \gg 1$), then it is possible to approximate the Lorentz factor in Eq. (16) by Dirac δ-function:

$$\frac{1}{1+\gamma_a^2(\Omega-\Delta)^2} \approx \frac{\pi}{\gamma_a}(\Omega-\Delta). \tag{17}$$

The resulting spectral perturbation is written as

$$\Re[\delta q(\Omega)] \approx \frac{\pi}{2\gamma_a}Gdz\, q_s(\Omega)g(\Omega). \tag{18}$$

Then $\delta\kappa$ and $\delta\Omega_s$ can be determined from Eqs. (14) and (15) as

$$\delta\kappa = \frac{\pi^2}{4\gamma_a}Gdz\int_{-\infty}^{\infty}\operatorname{sech}^2\left[\frac{\pi(\Omega-\Omega_s)}{2\kappa}\right]g(\Omega)\,d\Omega, \tag{19}$$

$$\begin{aligned}\delta\Omega_s &= \frac{\pi}{2\gamma_a}Gdz\\ &\quad\times\int_{-\infty}^{\infty}\frac{\pi(\Omega-\Omega_s)}{2\kappa}\operatorname{sech}^2\left[\frac{\pi(\Omega-\Omega_s)}{2\kappa}\right]g(\Omega)\,d\Omega.\end{aligned} \tag{20}$$

The form-factor increment $\delta\kappa$ is proportional to the overlap integral of the soliton spectral intensity $|q_s(\Omega)|^2$ with the amplification line spectral profile $g(\Omega)$. The soliton frequency variation $\delta\Omega_s$ is proportional to the first moment of the integral mentioned above.

When considering homogeneously broadened line we can use Eqs. (4), (10), and (12) and obtain that

$$\delta\kappa = \frac{\pi}{4}Gdz\int_{-\infty}^{\infty}\operatorname{sech}^2\left[\frac{\pi(\Omega-\Omega_s)}{2\kappa}\right]\frac{1}{1+\gamma_a^2\Omega^2}\,d\Omega, \tag{21}$$

$$\begin{aligned}\delta\Omega_s &= \frac{1}{2}Gdz\int_{-\infty}^{\infty}\left[\frac{\pi(\Omega-\Omega_s)}{2\kappa}\right]\operatorname{sech}^2\left[\frac{\pi(\Omega-\Omega_s)}{2\kappa}\right]\\ &\quad\times\frac{1}{1+\gamma_a^2\Omega^2}\,d\Omega.\end{aligned} \tag{22}$$

As in the previous case (Eqs. (19) and (20)) the soliton parameter variations may be determined as appropriate overlap integrals. This means that in the frame of the first-order perturbation theory, amplification of the femtosecond soliton basically does not depend on the broadening mechanism but only on the parameters and on the shape of the amplification line.

Let us return to the inhomogeneously broadened line and consider the physically relevant solutions which may be obtained as limiting cases of Eqs. (19) and (20). For a narrow band soliton ($\kappa/\tau_0 \ll 1/T_2^*$) one can use the approximations

$$\operatorname{sech}^2\left[\frac{\pi(\Omega-\Omega_s)}{2\kappa}\right] \approx \frac{4\kappa}{\pi}\delta(\Omega-\Omega_s), \tag{23}$$

$$\frac{\Omega-\Omega_s}{\kappa}\operatorname{sech}^2\left[\frac{\pi(\Omega-\Omega_s)}{2\kappa}\right] \approx \frac{2\ln 2}{\pi}[\delta(\Omega_s+\kappa/2)-\delta(\Omega_s-\kappa/2)], \tag{24}$$

and express the soliton parameters variations in the explicit form

$$\delta\kappa = \frac{\pi}{\gamma_a}\kappa g(\Omega_s) G dz, \tag{25}$$

$$\delta\Omega_s = \frac{\pi\ln 2}{2\gamma_a}\left(\frac{\partial g}{\partial\Omega}\right)_{\Omega_s}\kappa G dz. \tag{26}$$

Equation (25) predicts exponential growth of the form factor κ with the distance z. Equation (26) describes pulling of the pulse spectrum toward the gain peak or spectral self-trapping. The pulling strength is proportional to the slope of the amplification line contour $\partial g/\partial\Omega$ at the point $\Omega = \Omega_s$.

In the opposite case of a narrow amplification line (for example Gaussian line Eq. (7) in the limit $\sigma \to 0$) or a broadband soliton ($\kappa/\tau_0 \gg 1/T_2^*$) we have $g(\Omega) \approx \delta(\Omega)$ and Eqs. (19) and (20) reduce to

$$\delta\kappa = \frac{\pi^2}{4\gamma_a}\operatorname{sech}^2\left[\frac{\pi\Omega_s}{2\kappa}\right] G dz, \tag{27}$$

$$\delta\Omega_s = -\frac{\pi^2}{4\gamma_a}\Omega_s\operatorname{sech}^2\left[\frac{\pi\Omega_s}{2\kappa}\right] G dz. \tag{28}$$

The first of these equations predicts rather slow linear growth of the broadband soliton form factor κ with the distance z. The second one describes trapping of the pulse spectrum under the center ($\Omega_c = 0$) of a narrow amplification line. It is important to note that the restoring "force" at the right-hand side of Eq. (26) has the maximum value at the point $\Omega_s \approx \kappa/2$; it vanishes at the center of the amplification line ($\Omega_s = \Omega_c = 0$) and at the wings ($|\Omega_s| \to \infty$).

4. NUMERICAL SIMULATION

An analytical description which was presented in the previous section is valid only for adiabatic (slow on z) amplification of the one-soliton pulse. In our numerical experiments transformation of the pulse shape and its spectrum was analyzed by integrating Eqs. (1), (2), and (6) along the active fiber.

The split-step algorithm was used for numerical integration of the nonlinear Schrödinger equation. It allows us to calculate the complex amplitude q on each z step as a result of the successive application of operators describing dispersion pulse spreading, the self-phase modulation, amplification and Raman self-frequency shift. The spectral approach was used to calculate the dispersion spreading. Integration of the equations for molecular oscillations and active ion polarization was also accomplished by the spectral method based on the fast Fourier transform algorithm. For calculation of the active ion polarization the integral in Eq. (6) was approximated by the sum of Lorentzian lines (Eq. (4)) with the weight factors corresponding to the amplification line contour $g(\Omega)$.

In numerical experiments we usually take a pulse of the form

$$q(0,\tau) = \operatorname{sech}(\tau)\exp(i\Omega_0\tau) \tag{29}$$

as the initial condition, where Ω_0 is the normalized by τ_0^{-1} detuning between the pulse initial carrier frequency and the gain peak frequency.

To visualize dynamics of the femtosecond soliton amplification we present the phenomenological picture of such a process. Figure 1a shows the evolution of the pulse shape during nonadiabatic amplification. Notice that the growth of the soliton amplitiude results in decreasing of its duration and consequently stimulates the red self-frequency shift (see also Eq. (9)). Increasing of the group delay due to the self-frequency shift is quite obvious in a time domain. One can also see that a new pulse appears at the second half of the propagation distance.

The pulse spectrum evolution can help us to understand the physics of the process. In Fig. 1b the spectrum of the amplified soliton is shown for different z. It is clear that the main soliton component of the spectrum broadens, shifts to the lower frequency region, and leaves the contour of the amplification line almost completely at the end of propagation distance. The amplification process stops and the soliton form factor reaches its stationary value but the carrier frequncy continues to shift into the red spectral region. One can also observe a new spectral cluster appearing under the amplification line. In a time domain it corresponds to the new pulse. Notice that the same phenomena are observed during amplification in a fiber with homogeneously broadened line [6] provided that saturation is negligible. We have used the inverse scattering transform method [10] for analysis of the complicated wave packets obtained as the result of numerical integration (see for example Fig. 1a). It gives possibility to determine the number of solitons within the composed wave packet and also to calculate their parameters κ, Ω_s.

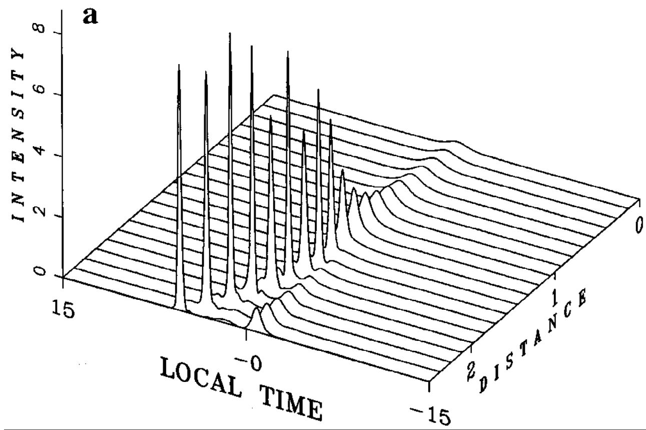

(a)

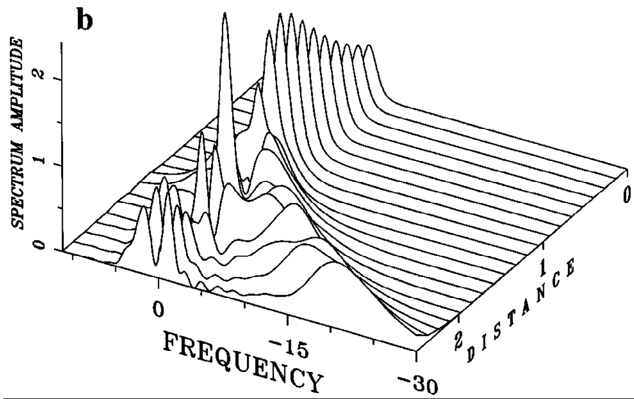

(b)

FIG. 1. Temporal (a) and spectral (b) evolution of the soliton pulse in an amplifier with IBL. The graphs were obtained by numerical integration of Eqs. (1), (2), and (6) with the initial condition Eq. (29). Parameters: $G = 4$, $L_F = 2.5$, $\Omega_0 = 0$, $\sigma = 4.25$, $\gamma_a = 1$, $\mu = 0.125$, $\delta = 0.28$.

It is interesting to compare the amplification dynamics for both kinds of the broadening mechanism quantitatively. In the case of HBL the numerical integration is related to Eqs. (1), (2), and (3) with the initial condition Eq. (27). We have chosen IBL and HBL lines with equal widths and peak gain coefficients. First we considered the case $\Omega_0 = 0$ when the initial carrier frequency of input pulse corresponds to the peak of the amplification line and assumed that the product GL_F remains constant (L_F is the fiber length). This allows the possibility for comparing adiabatic and nonadiabatic regimes of amplification. The resulting dependencies of the output form factors $\kappa(L_F)$ on the amplification coefficient G which were calculated by the inverse scattering method are shown in Fig. 2 for the cases of homogeneously and inhomogeneously broadened lines. Notice that large values of G correspond to nonadiabatic amplification which is not managed by the perturbation theory. For example one can observe the appearance of the second soliton pulse for $G > 0.3$. From Fig. 2 it is clear that the soliton under IBL is amplified more effectively (by 8–10% approximately) in comparison with the HBL. This

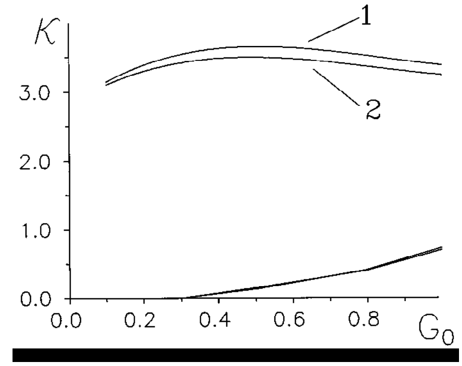

FIG. 2. Dependence of the output soliton form factors on the amplification coefficient G for both kinds of broadening mechanisms: IBL (1) and HBL (2). Parameters: $GL_F = 1$, $\mu = 0.125$, $\delta = 0.28$; IBL $- \sigma = 4.25$, $\gamma_a = 1$; IBL $- \gamma_a = 0.2$.

fact may be attributed to the difference of the lines shapes and to the higher order perturbation effects.

We also considered the carrier frequency shift in dependence on the amplification parameter G. These results are presented in Fig. 3. From the graphs one can conclude that for both kinds of the amplification line broadening mechanisms the self-frequency shift is approximately the same. The output value of $\Omega_s(L_F)$ increases with decreasing of G because the product GL_F was fixed and for a long fiber the Raman self-frequency shift is more pronounced.

In the next series of computer simulations we studied the dependence of the output form factor on the initial soliton frequency Ω_0. These results are presented in Fig. 4. From this figure one can conclude that IBL amplifier is more effective than HBL one. Maximum value of the output form factor is reached at $\Omega_0 \simeq 1.5$, i.e., when the initial carrier frequency of the soliton is on the anti-Stokes wing of the amplification line. This means that the amplification is enhanced in the case when the soliton carrier frequency scans across the whole amplification line contour due to the Raman self-frequency shift.

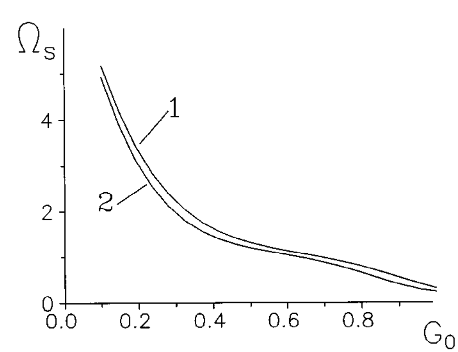

FIG. 3. Dependence of the output soliton self-frequency shift $\delta\Omega_s$ on the amplification coefficient G for both kinds of broadening mechanisms: IBL (1) and HBL (2). Parameters: $GL_F = 1$, $\mu = 0.125$, $\delta = 0.28$; IBL $- \sigma = 4.25$, $\gamma_a = 1$; IBL $- \gamma_a = 0.2$.

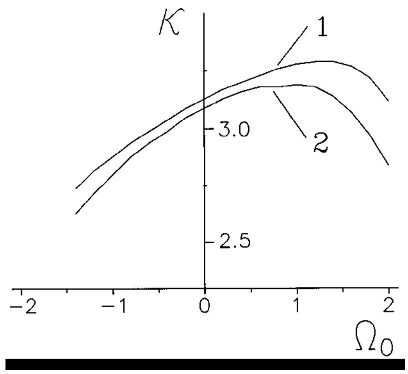

FIG. 4. Output soliton form factors as functions of the initial frequency detuning Ω_0 for both kinds of broadening mechanisms: IBL (1) and HBL (2). Parameters: $G = 0.1$, $L_F = 10$, $\mu = 0.125$, $\delta = 0.28$; IBL$-\sigma = 4.25$, $\gamma_a = 1$; IBL $- \gamma_a = 0.2$.

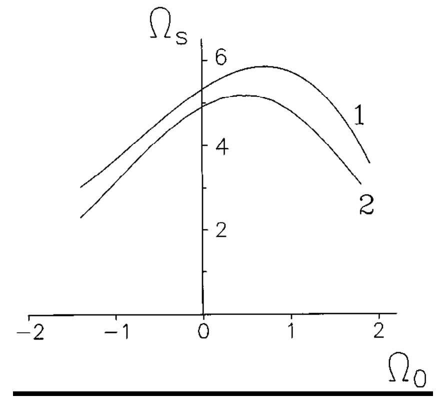

FIG. 5. Output soliton self-frequency shifts $\delta\Omega_s$ as functions of the initial frequency detuning Ω_0 for both kinds of broadening mechanisms: IBL (1) and HBL (2). Parameters: $G = 0.1$, $L_F = 10$, $\mu = 0.125$, $\delta = 0.28$; IBL$-\sigma = 4.25$, $\gamma_a = 1$; IBL $- \gamma_a = 0.2$.

The output Raman self-frequency shift $\Omega_s(L_F)$ in the case of adiabatic amplification is shown in Fig. 5 as a function of Ω_0. Maximum of the $\Omega_s(L_F)$ is reached at the point $\Omega_0 \sim 1$, which corresponds to the maximum of the form factor; this is quite natural because the Raman self-frequency shift strongly grows with κ.

5. CONCLUSION

In conclusion we would like to emphasize that the Raman self-frequency shift is one of the most important factors which limits the amplification of femtosecond solitons in IBL and HBL active fibers. The physical mechanism of the line broadening does not affect significantly on the femtosecond soliton amplification provided that the lines contours are similar and saturation effect is negligible. Appreciable enhancement of the amplification factor can be achieved in the case when the initial carrier frequency of the soliton is on the anti-Stokes wing of amplification line or a broadband line is used. In our opinion the spectral perturbation method presented in this paper is very useful for analysis of the ultrashort soliton propagation.

ACKNOWLEDGMENT

This work was partially supported by CONACyT through the program “Cátedras Patrimoniales de Excelencia, nivel II”.

REFERENCES

[1] E. Desurvire, *Erbium doped fiber amplifiers; principles and applications*, Wiley, New York, 1994.

[2] G. P. Agrawal, *Fiber optic communication systems*, Wiley, New York, 1992.

[3] R. J. Mears and S. R. Baker. “Erbium doped fiber amplifiers and lasers,” *Opt. Quantum Electron*. vol. 24, 517 (1992).

[4] K. Kurokawa and M. Nakazawa, “Wavelength dependent amplification characteristics of femtosecond erbium doped optical fiber amplifiers,” *Appl. Phys. Lett*., vol. 58, no. 25, 2871 (1991).

[5] D. J. Richardson, V. V. Afanasjev, A. B. Grudinin, and D. N. Payne, “Amplification of femtosecond pulses in a passive, all-fiber soliton source,” *Opt. Lett*., vol. 17, no. 22, 1596 (1992).

[6] V. V. Afanasjev, V. N. Serkin, and V. A. Vysloukh, “Amplification and compression of femtosecond optical solitons in active fibers,” *Sov. Lightwave Commun*., vol. 2, no. 1, 35 (1992).

[7] E. Marti-Panameño, J. J. Sanchez-Mondragon, and V. A. Vysloukh, “Theory of the soliton pulse forming in an actively mode-locked fiber laser,” *IEEE J. Quantum Electron*., vol. QE-30, no. 3, 822 (1994).

[8] G. P. Agrawal, *Nonlinear Fiber Optics*, Academic Press, San Diego, 1995.

[9] F. M. Mitshke and L. F. Mollenauer, “Discovery of the soliton self-frequency shift,” *Opt. Lett*., vol. 11, no. 10, 659 (1986); J. P. Gordon, “Theory of the soliton self-frequency shift,” *Opt. Lett*., vol. 11, no. 10, 662 (1986).

[10] V. A. Vysloukh and I. V. Cherednik, “On the restricted N-soliton solutions of the nonlinear Schrödinger equation,” *Theoret. Math. Phys*., vol. 71, no. 1, 13 (1987); S. A. Akhmanov, V. A. Vysloukh, and A. S. Chirkin, *Optics of Femtosecond Laser Pulses*, Chap. 5, American Institute of Physics, NY, 1992.